Subsidence, Fault Activation and Groundwater Production in The Woodlands

Neil Gaynor
MUD 6 President

During the August 11 Woodlands Water Agency (WWA) Trustee meeting, two members of the public provided comment on drainage and property impacts due to general subsidence and differential subsidence (fault related) caused by groundwater production. The issue of subsidence mitigation by adjusting the relative proportion of surface water to groundwater supply was also commented upon. During the meeting, these issues were discussed by the Trustees and the WWA General Manager, Jim Stinson, requested wording for a future agenda item for the next Trustee meeting. I have prepared this document to provide some background for that agenda item.

1. Public Comment Summary

Dr. Meinrath discussed issues regarding faulting at his home, causing the northwest part of his residence to fall about 0.5 inches per year since 1992. Dr. Meinrath noted a reduction in the rate of movement on the fault following implementation of the Groundwater Reduction Plan (GRP) and the supply of surface water to The Woodlands. He requested that WWA Trustees support analysis of the fault by an independent professional geologist. [Note: I have met with Dr. Meinrath to receive information from him to better understand this issue. The fault passing under his residence is known as the Panther Branch Fault (Figure 1). This fault trends approximately east-northeast and shows a displacement down to the northwest. It passes through the intersection of Research Forest and the entrance to The Woodlands High School. The fault is visible in the student parking lot on the west side of the entrance.]

Mr. Unland expressed concerns about the relative proportion of surface water to groundwater (SW/GW) and its impact on drainage due to subsidence. He noted that the current budgeted blend ratio of the two sources is 35/65. However, the higher initial blend ratio when the GRP was implemented appeared to limit subsidence because of reduced groundwater production. Mr. Unland noted that he had not seen information from the trustee board concerning an alternative 50/50 blend ratio, although such a request has been made in the past.

2. Known Faults in The Woodlands

The map shown in Figure 1 depicts the general locations of known faults in The Woodlands. The locations are derived from past studies by consultants for SJRA and Woodland residents, and my own reconnaissance mapping (see under section 5 for the consultants' names).

The named faults from northwest to southeast are Egypt, Big Barn, Jones, Panther Branch and Navarro. Although the faults are shown as simple lines on the map, in reality these faults may be segmented or offset in an *en échelon* pattern. These features are the surface expression of the Hockley-Conroe Fault System, which was first recognized in the 1930s. In turn, this system

is a minor part of a coast-parallel system of growth faults extending from Louisiana to the Texas-Mexico border.

The Texas coastal plain is the landward margin of the Gulf of Mexico Basin and is underlain by a seaward thickening sediment wedge comprising sand, gravel and mudrock lithologies, all of which become increasingly lithified or compacted with depth. Growth faults are common structural features found in the sedimentary fill on the margin of Gulf of Mexico Basin where there is active deposition over a relatively mobile substrate, such as salt beds or over-pressured shales known from seismic imaging and oil-well drilling deep under the Texas coastal plain and offshore areas. Two key characteristics of growth faults are their listric geometry, where fault dip decreases with depth, and thickening of sediment fill on the downthrown side of these faults.

In recent years, remote sensing techniques have been used to help locate the surface expression of growth faults. LiDAR (Light Detection And Ranging) is one such technique used to detect fault offset at the ground surface. A 2013 University of Houston study identified the location of the Big Barn Fault in The Woodlands and the northern extension of the Hockley Fault (Figure 2). A later study by Southern Methodist University (discussed below in section 5) utilizing Interferometric Synthetic Aperture Radar (InSAR) provides much greater detail on this and related faults in The Woodlands.

Although growth faults may show surface expression as a natural geologic process independent of anthropomorphic activities, there is the potential of activation of these faults by such activities, including the production of groundwater.

3. Groundwater Pumping and the Subsidence Mechanism

Since the 1920s, soil and hydrocarbon reservoir geomechanics studies have shown that the mechanical response to overburden stress within sediments, including aquifers, comprises two components (Zoback, 2007, p. 66). [Reference: Zoback, M.D., 2007, Reservoir Geomechanics, Cambridge University Press, 449 pp.]

Overburden stress is simply the pressure (force per unit area) due to the gravitational force exerted by the mass of geological sediments and contained fluids (principally water) at an arbitrary location below the surface. The two components of force resisting the overburden stress are effective (matrix) stress and fluid pressure within the sediment pore space. In equation form,

$$\sigma_T = \sigma_e + p$$

where σ_T = total overburden stress
σ_e = effective (matrix) stress
p = pore pressure

If fluid pressure in the pore space is reduced by pumping groundwater, the resistance to the overburden stress must be balanced by an increase in effective stress. In aquifers having high

compressibility due to the presence of clay layers, the higher matrix stress will result in deformation and compaction (Figure 3A).

When groundwater is pumped from an aquifer, preferential production is from coarse-grained layers, such as sands and gravels, which generally have high transmissibilities. A pressure differential is set up between the coarse-grained and fine-grained layers (situation 1 in Figure 3A). As a result, there is flow into the coarse-grained layers as shown by the blue arrows in Figure 3A. As water flows from the fine-grained layers, effective (matrix) stress increases in these layers (situation 2 in Figure 3A).

This outward flow is one-time and one-way, which leads to rearrangement and compaction of the clay and silt matrix (Figure 3B). The fine-grained layers, being highly compressible, have insufficient mechanical strength to carry the overburden load as a result of the increased effective stress (situation 2 in Figure 3A). Irreversible rearrangement and compaction of the clay and silt layers will continue until the matrix material can support the increased effective stress.

As the fine-grained layers compact, the land surface will subside (situation 2 in Figure 3A). Because nearly all of the irreversible compaction of the aquifers will be in the fine-grained layers, subsidence is also irreversible.

4. Measurement of Subsidence and Fault Displacement

Past concerns regarding subsidence due to groundwater pumping from the Gulf Coast Aquifer underlying the upper Texas coastal plain had led to the establishment of the Harris-Galveston Subsidence District (HGSD) in 1975. This special district has regulatory control over groundwater pumping and monitors subsidence to assess the efficacy of pumping limitations. HGSD measures subsidence using traditional surveying techniques, extensometers (for measuring compaction), GPS stations (both continuous and periodic), and satellite remote sensing via InSAR. The most accessible data with the widest coverage comprises GPS measurements, either Continuously Operating Reference Stations (CORS) managed by the National Geodetic Survey or Port-A-Measure (PAM) stations established by the HGSD in Harris and surrounding counties.

Within The Woodlands, several studies provide documentation of elevation changes in the recent past. These studies include all of the measurement types discussed in the previous paragraph, with the exception of extensometer instrumentation.

The PAM 13 (also designated P013) station has the longest record of subsidence measurements, beginning in late 2000 (Figure 4). This station is located near to SJRA's Wastewater Treatment Facility No. 2 off Research Forest Drive. Data are recovered from this station periodically and analyzed by the University of Houston to ensure consistency with current reference framework information. The data are then published on the HGSD website as part of their annual reporting requirements.

P013 data clearly show subsidence of over 20 cm between late 2000 and 2015. In late 2015, treated surface water from Lake Conroe became available to The Woodlands as part of SJRA's Groundwater Reduction Plan (GRP). In turn, groundwater pumping in The Woodlands was reduced and subsidence appeared to stabilize over the period 2016-2019. Unfortunately, the previous subsidence trend appears to have become re-established in the 2019-2020 timeframe.

The SJRA Woodlands Division presented information to Woodlands Water Agency and The Woodlands MUDs which suggests a close relationship between The Woodlands groundwater pumping rates (expressed as the surface water/groundwater blend ratio) and land subsidence (Figure 5). The data presented is a subset of PAM13 elevation change over the period 2010 to the start of 2020. Between 2010 and late 2015, slightly less than 10 cm of subsidence was measured. With the availability of surface water blended in the ratio 65/35 to 50/50 SW/GW, subsidence appeared to stabilize until the start of 2019. With reduction of the ratio to 35/65 SW/GW, i.e., greater relative groundwater pumping, an increase in subsidence is indicated. The compaction sensitivity of the Evangeline and Jasper Aquifers to groundwater pumping appears to have confirmation in the P013 subsidence data.

SJRA has a fault monitoring program in operation in The Woodlands at three locations along Research Forest Drive, from the intersection with FM 2978 to The Woodlands High School, where the Egypt, Big Barn and Panther Branch Faults cross this road (Figure 6A). The monitoring comprises periodic resurveys of benchmarks to determine if there could be the potential for damage to the GRP pipeline due to differential ground movement across these faults.

Reports and data from the monitoring locations are found on the following website: https://www.sjra.net/grp/fault-monitoring/ The current monitoring report suggests no fault activity on any of the three faults since 2015, after the pipeline was laid. However, the report goes on to state that at Segment W2A, at the intersection of Research Forest and Cats Cradle Drives, "there is evidence that the western segment of the transect has dropped more than the eastern segment of the transect." The survey area is shown in Figure 6B with the western and eastern benchmarks indicated by their respective colors. The estimated surface location of the Panther Branch Fault is shown by the dotted line.

CORS stations in The Woodlands also provide useful information on subsidence, although the period of measurement is much less than the P013 station. An example from the WHCR station at The Woodlands High School, which is located south of the intersection of Research Forest and Cats Cradle Drives, is shown in Figure 7A. This station is 0.92 miles (approx. 1.5 kilometers) west of P013.

The period of measurement starts in early 2015 and runs through mid-2021. Relative to the IGS14 reference frame (see link to Nevada Geodetic Laboratory on Figure 7A), a subsidence rate of 0.86 cm/year has been calculated. The WHCR station also measures the horizontal motion of the North American tectonic plate as presented in the Figure 7B.

Unlike the P013 station data, no clear evidence of stability of the subsidence rate is evident, except possibly in the period 2016-2017. Finally, a clear periodicity is evident in the North-South and vertical axes. A subdued periodicity is also present in the East-West axis. This periodicity on millimeter scales is likely due to seasonal atmospheric and hydrologic effects, although further investigation should be undertaken to account for this phenomenon.

For direct measurement of deformation on the Panther Branch Fault, Dr. Meinrath provided information on multiple engineering surveys at his residence (Figure 8). The consultants responsible for the work performed detailed elevation surveys of the foundation to determine the geometry of the flexure related to differential subsidence across the fault relative to a fixed corner point, R. The estimated surface trace of the fault is shown by the diagonal double arrow line across the upper section of the residential plan.

The slab foundation shows increasing deformation towards point A (to the northwest). Two profiles along the section line from reference point R to point A for the years 2001 and 2006 are to the right of the residence plan. Dr. Meinrath has summarized the ongoing displacement at point A in the table shown at the bottom of the figure. The range of change per year in elevation increases from 0.42 in/year (1 cm/year) in 1992 to 0.70 in/year (1.8 cm/year) in 2013. A major slowdown in the subsidence rate over the period 2013 to 2020 averaging 0.18 in/year (0.5 cm/year) shows similarities to the P013 subsidence data.

5. Remote Sensing of Regional and Differential Subsidence

The examples of subsidence measurements discussed in Section 4 provide limited lateral information on regional subsidence and differential deformation along faults. To build a picture of surface elevation changes over larger scales, remote sensing techniques are required.

InSAR is an emerging technique for detailed, rapid assessment of elevation changes. Satellites in low earth orbit scan the surface of the Earth making multiple recordings of reflected radar energy along the track of the orbit (hence the term synthetic aperture). With multiple passes over the same area, a time series of radar reflections can be assembled. The phase information contained in the reflected radar signals is used to make measurements of the distance of the satellite to the surface. By comparing successive phase changes in the reflected radar energy interferograms can be constructed. These are then used to calculate changes in surface elevation. The accuracy of these changes is in the centimeter to sub-centimeter (millimeter) range. Details of this technique can be found at the NASA website https://earthdata.nasa.gov/learn/backgrounders/what-is-sar

Although some InSAR studies have been conducted in the Greater Houston area only one, to the author's knowledge, published in 2019, has been targeted to make detailed analyses of subsidence in The Woodlands. [Reference: Qu, F., Lu, Z., Kim, J-W., and Zheng, W., 2019, Identify and Monitor Growth Faulting Using InSAR over Northern Greater Houston, Texas, USA, Remote Sensing, 11, 1498, p. 1-23.]

The authors utilized a multi-temporal InSAR technique to measure subsidence and fault movement in The Woodlands. The data set comprises L-band Advanced Land Observing Satellite (ALOS) radar tracks acquired over the period 2007-2011. L-band radar has a frequency of 1-2 GHz with a corresponding wavelength range of 30-15 cm. This radar band has limited atmospheric absorption, high penetration in forested regions and is most useful for InSAR analysis.

InSAR deformation rates are shown by colored pixels on the map of the Greater Houston area (Figure 9A1) with negative values show by warm colors (yellow through red) and positive values shown by cool colors (green through blue). Negative values indicate subsidence. It is noteworthy that the largest negative values are in areas known to have substantial groundwater withdrawal rates, including The Woodlands, Spring and northern Harris County, northwest Harris County, and the Katy area. It is important to note that in areas with lower groundwater pumping rates, subsidence is negligible, including eastern and northern Montgomery County. In the recent past, claims have been made by Lone Star Groundwater Conservation District (LSGCD) that Harris County groundwater pumping has caused subsidence in Montgomery County. This InSAR-derived deformation map refutes that claim, certainly during the period of data acquisition.

The focus area of the study is enclosed by the dashed purple line. This area is enlarged in Figure 9A2. The enlargement provides a clearer depiction of subsidence and fault complexity in this area, including a newly discovered fault complex between Conroe and Magnolia (near the end of section line P2-P2').

Figure 9B shows a profile of several parameters along the section line P2-P2'. The section line runs northwest to southeast and the distance along the profile is shown at the bottom of the graphic. Starting with the uppermost curves, two displacement gradients from ALOS tracks 175 and 176 (light and dark blue lines respectively) are shown. The scale for the displacement gradient is on the right in units of mm/pixel. Although not specified in the Qu, et al. paper, the pixel resolution is approximately 10-20 meters (see Figure 10B). As expected, displacement gradient changes are most evident at fault locations.

The next lower set of curves comprise surface displacement rates determined from the two ALOS data sets (light grey – track 175, black – track 176). The scale is on the left with units of mm/year. The increase in subsidence between the two fault traces of the Big Barn Fault complex is evidence of activity on these faults (see note on fault nomenclature in the figure caption).

The yellow line shows the elevation profile along the section line, with the scale in meters on the left. This scale is insufficient to show changes in surface elevation due to fault activity. Finally, geophysical studies by Qu, et al., have estimated rates of movement and the geometry of the Conroe and Egypt Faults in the subsurface (bottom panel in diagram). Note the

difference in horizontal and vertical scales. The length of arrow in the legend on the right provides a scale for rates of motion on these faults.

Calibration of the InSAR subsidence rates in The Woodlands and those determined using GPS measurements at the PAM 13 station is shown in Figure 9C. The temporal changes in elevation over the period 2017 to 2011 (red dots) agree well with the PAM 13 data set. Incidentally, the change in subsidence rate measured at PAM 13 following lower groundwater pumping rates in The Woodlands in late 2015 is evident. Five other GPS stations (rod1, PAM 11, PAM 17, PAM 18, and PAM 48) show similar levels of agreement with the InSAR subsidence measurements (see Qu, et al., Figures 1 and 7).

Focusing on subsidence in The Woodlands and centered on the Big Barn Fault system, Qu, et al., have integrated geologic field observations and remote sensing deformation data into a single display (Figure 9A). The color display range for deformation rates has been expanded from that in the previous map to highlight fault offsets. However, this change has had the unfortunate consequence of color saturation for deformation rates in the range -12 to -40 mm/year in The Woodlands east of Lake Woodlands (LW on Figure 10A). Qu, et al., have not clearly stated which data set is used for the deformation rate map. It is assumed it is the merged InSAR data from ALOS tracks 175 and 176.

Fault offsets have been confirmed in the field by Fugro Consultants, Inc. (FCI), Tolunay-Wong Engineers, Inc.(TWEI), and Qu, et al. The FCI and TWEI fault scarp locations are shown by the grey and green symbols, respectively. Qu, et al. confirmed fault scarps at two locations shown by the stars. In addition, interpreted fault traces from FCI, TWEI, LiDAR and InSAR are shown (refer to the legend).

The blue box in Figure 10A corresponds to the location of the InSAR deformation rate map shown in Figure 10B. Qu, et al., appear to have either used a decimated merged InSAR data set or data from ALOS track 176. The pixel color range corresponding to deformation rates is different to that in Figure 10A. Nevertheless, the fault offset on the Big Barn Fault is clearly evident, with upthrown and downthrown sides demarcated. This inset map is from the western part of The Woodlands. The North arrow on the left side of the image will help with orientation of Figure 10B. In addition, the intersections of Research Forest Drive, Greenbridge Drive and SH 242 on the right side of the image are useful landmarks. Qu, et al., have not designated the Panther Branch Fault on this map, but it is located along the boundary (lower right-hand side of image) where there is an abrupt change from high deformation rates (orange and red pixels) to low deformation rates (green pixels).

6. Discussion of the Impacts of Aquifer Depletion and Land Subsidence

Groundwater pumping which depletes aquifers has multiple impacts, only some of which are evident until after irreversible damage has been done. A subtle impact is the permanent loss of storage capacity in the aquifer mostly in fine-grained layers, which typically have low transmissibility rates. Storage capacity refers to the volume of water that can occupy the pore

space of an aquifer. That our aquifers are being depleted is clearly evident by the decline in water levels regularly reported by SJRA in groundwater production wells. It is only with the introduction of an alternative surface water source that the drop in aquifer water levels has slowed.

Another impact relates to the cost of producing groundwater. As aquifers decline, the remaining groundwater must be lifted higher to the surface. This means that pumps will require more energy to move the water up the tubing of the wells. Eventually, if the decline becomes sufficiently large, wells will need to be recompleted deeper or replaced, adding more costs.

With ongoing groundwater production, a reduction of groundwater contribution to river and stream flow will follow. When there has been little rainfall, much of the water in flowing comes from groundwater seepage. Interception of groundwater by water well production, especially during drought, will cause a loss of riverine flow.

However, a most consequential impact of groundwater depletion, especially to property, is compaction of aquifers and surface subsidence. As the PAM13 data show, the Evangeline and Jasper Aquifers appear to be sensitive to pumping rates. An almost immediate stabilization of subsidence by reduced groundwater pumping is clearly evident.

Surface subsidence, in turn, will likely have the following consequences, which have been seen in Harris County, and which are emerging in Montgomery County. These are changes in drainage patterns, worsening flood impacts, and fault activation. Relative attribution of surface deformation due to groundwater depletion or on-going growth faulting is challenging and requires more study. However, the evidence of change in fault activity related to lower groundwater pumping (from Dr. Meinrath's data) is compelling.

The subsidence impacts are all physical effects related to groundwater pumping. These physical effects translate into property value impairment by increasing flood damage risk to residences, businesses, and infrastructure. In addition, fault activation may impact such entities, but the effects of such movement on fault surfaces are laterally limited to areas of offset. However, if fault systems become activated, resulting in relative lowering the land surface, flood damage risk may increase. All of these physical effects are likely to result in reduced property values and lower property tax receipts.

One of the major challenges in assessing the implications of declining groundwater levels is a quantitative assessment of the amount of subsidence related to lowered groundwater levels. This issue is complicated by groundwater production from two aquifers, the unconfined Evangeline Aquifer, and the confined Jasper Aquifer, separated the Burkeville confining unit. Therefore, the partitioning of aquifer compaction to determine total subsidence is needed.

One major problem to address is that the unintended consequences of groundwater pumping, namely property, flood, and infrastructure damage due to subsidence and fault activation are

treated as externalities or unaccounted-for costs. A case in point is the determination GRP surface water/groundwater mix supplied to those GRP participants receiving surface water. Devaluation of property and infrastructure replacement costs due to increased flood risk and fault movement are not part of the criteria for managing groundwater extraction rates.

7. Summary and Recommendations

In my opinion, the public comments of the two residents at the August 11 Woodlands Water Agency Trustee meeting provide a fair critique of the present approach to surface water/groundwater management in The Woodlands. It is likely that major hurdles will hinder changes to current policies and practices, however, the costs to be borne by some residents and governmental entities in The Woodlands should no longer be treated as simple externalities. It should be possible to optimize surface water and groundwater sources to meet future consumer demand, but not at the cost of further damage to property and infrastructure.

Some key questions to be addressed are these:
What are the maximum groundwater volumes to be pumped from the Evangeline and Jasper aquifers to meet both water demand in The Woodlands and still minimize subsidence and fault activation?
What should be the maximum allowable subsidence over the next 20-, 40-, 60-year periods?
If The Woodlands reduces groundwater pumping, what is the risk of groundwater depletion, with its attendant subsidence and faulting issues, caused by pumping in adjacent areas?
What is the notional consumer cost trajectory, in $/1000 gallons, related to provision of larger volumes of surface water?

Recommendations for action to address groundwater production and subsidence issues that may be made herein will overlap with, and will be redundant in part, to those already articulated by the Groundwater Science Advisory Committee (SAC) in their two reports to the Regional Groundwater Science Partnership and other stakeholders. [References: Reference (1) Groundwater Science Advisory Committee (2021), Review and Recommendations on "Subsidence Investigations – Phase 1" Report. Prepared for the Regional Groundwater Science Partnership, Houston Advanced Research Center, The Woodlands, Texas, 14 pp., and Reference (2) Groundwater Science Advisory Committee (2021), Guidance for Monitoring Land Subsidence in Montgomery County, Texas, Houston Advanced Research Center, The Woodlands, Texas, 20 pp.]

The proposed approach by SAC (see p. 15 of Reference 2) recommends "an integrated approach to evaluation current and historical groundwater resources and subsidence in Montgomery County." Such a challenging goal will only be achieved through cooperative partnerships and sharing of expertise to uncover the scientific underpinnings of the relationships between subsidence, fault activation and groundwater pumping. Given that two detailed reports are already available, it would seem that the logical extension of this recommendation is for the Houston Advanced Research Center (HARC) to provide the lead role for management, coordination, and reporting.

I believe the WWA Trustees and other stakeholders should consider, in addition to the SAC reports, the following recommendations for undertaking an integrated evaluation of groundwater pumping, faulting and subsidence:

1. Expand the Regional Groundwater Science Partnership to include diverse and willing stakeholders, by inviting the Houston-Galveston Subsidence District, Lone Star Groundwater Conservation District, One Water Task Force, San Jacinto River Authority, and other GRP participants to join.
2. Review the new GULF-2023 groundwater flow model, currently being built by the US Geological Survey. This model is expected to be completed by the end of 2021, and once accepted by the Texas Water Development Board and Houston-Galveston Subsidence District, will replace the current Houston Area Groundwater Model (HAGM). Residents and governmental entities in the northern part of the Gulf Coast Aquifer System have a clear stake in the reliability of the GULF-2023 model. Reference: https://www.twdb.texas.gov/groundwater/models/gam/glfc_n/glfc_n.asp
3. Request updates from the Houston-Galveston Subsidence District on two key studies that are currently underway, quoting from SAC report (Reference 2 above): "Mapping Land Deformation over Houston- Galveston Using Multi-temporal InSAR Processing" (2020–2021), which uses InSAR combined with other data to produce yearly deformation maps over the Houston-Galveston region from 2004 to 2020 and "Evaluation of Subsidence Impacts on Spring Creek Watershed (2020-2022)," which will examine subsidence impacts on the Spring Creek Watershed.
4. Explore building a GIS database to capture and visualize flood and fault impacted locations in The Woodlands, including changes in property valuations made by the Montgomery County Central Appraisal District.
5. Engage a structural geologist and specialist in geomechanics to assess the physical controls for activation of growth faults in the shallow subsurface due to aquifer pressure reduction. An important additional assessment is the attribution of near-surface fault movements due to natural geologic processes versus groundwater pumping.
6. Develop a robust methodology for policy- and decision-making under uncertainty absent complete information on required research, and data acquisition and analysis. A particular focus should be to address issues that are currently externalities such as risk for property damage that may be caused to the unintended consequences of groundwater production.

Disclaimer

The opinions and ideas expressed herein are protected by the First Amendment of the US Constitution and the Anti-SLAPP Statute of the State of Texas. Materials in this document are retrieved from private, public domain, and on-line sources. Fair use is claimed for non-profit educational and research purposes. All information is for general informational purposes only and is provided in good faith. The author makes no representation or warranty of any kind, implied or expressed, regarding the accuracy, completeness, adequacy, reliability, or availability of the information in this document. The author will not be held responsible for any use of information contained in this document. If specific advice on the content of any part of this document is needed, consultation with a professional who is qualified and licensed in the appropriate area of expertise is strongly recommended.

The original of this document was generated using Microsoft Word. Microsoft Word Editor has determined that 0% of the text in this document is similar to online sources.

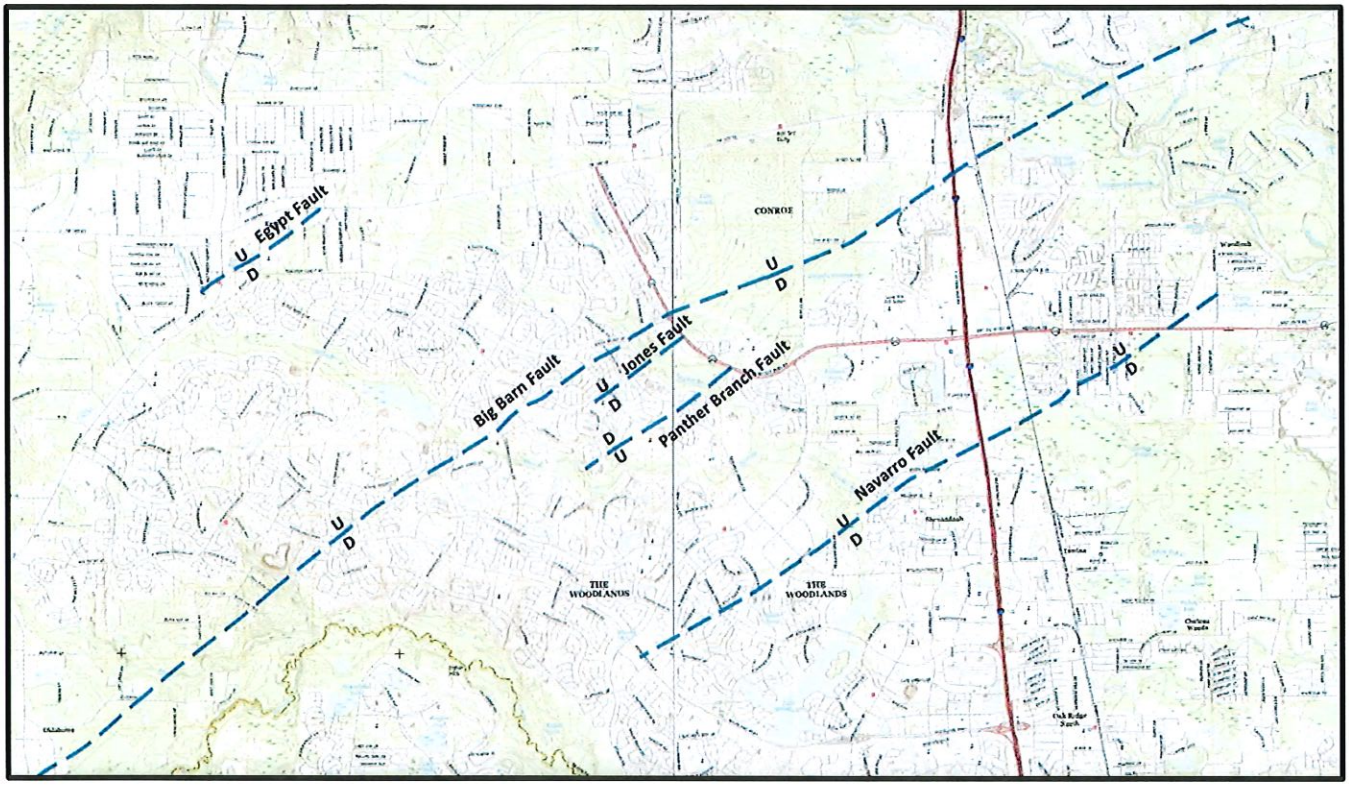

Figure 1. Fault map of The Woodlands with named faults and sense of movement (U = up; D = down). The base map was made by merging parts of the USGS 7.5-minute topographic series, Tamina and Oklahoma Quadrangles, 2016 vintage.

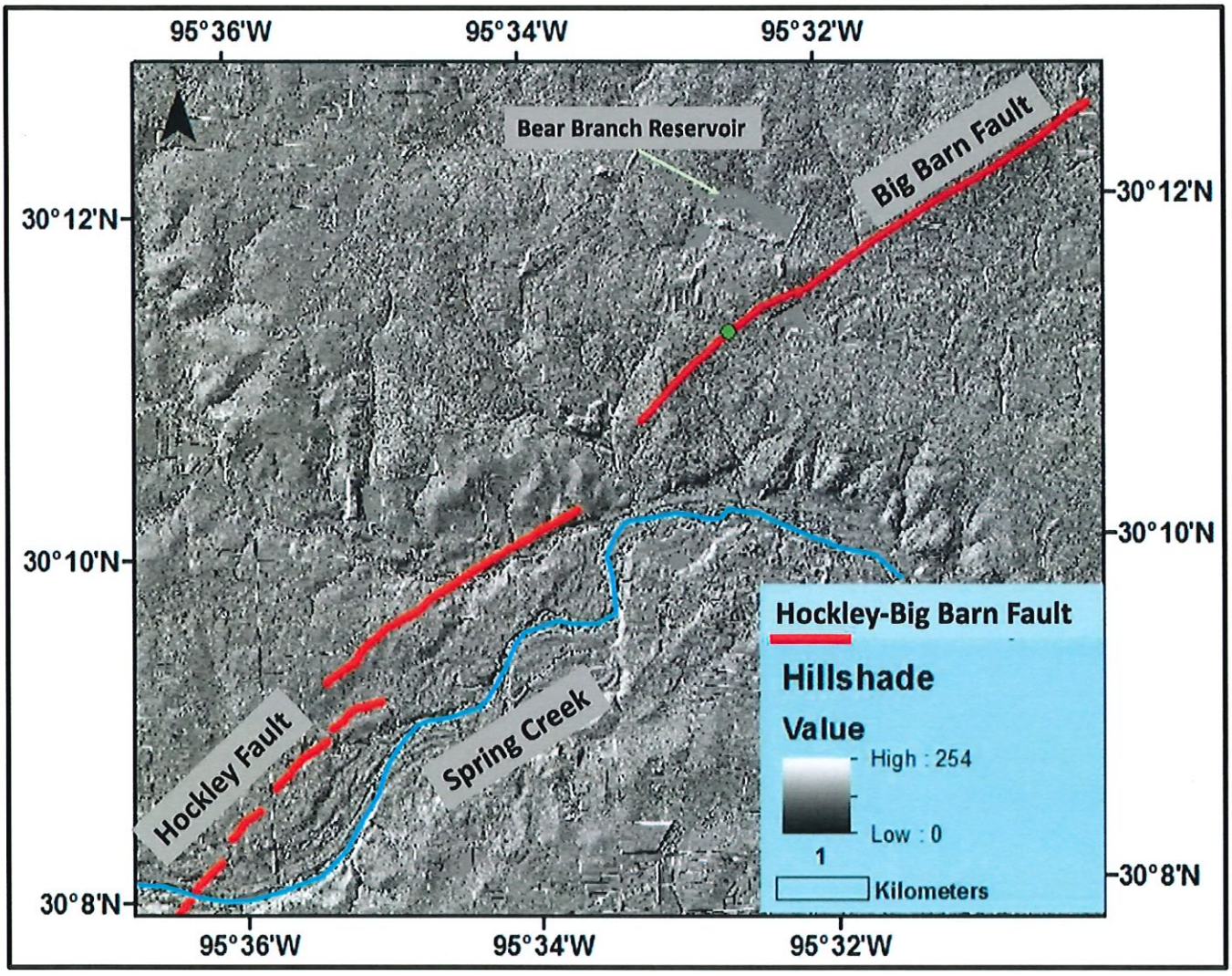

Figure 2. LiDAR image of the Hockley-Big Barn Fault system in The Woodlands and adjacent areas. Key geographic elements are identified for reference. Image modified from Figure 3.11 in Han, X., 2013, Integrated Remote Sensing and Geophysical Study of the Hockley Fault in Harris and Montgomery Counties, Texas, University of Houston, MS thesis, 72 pp.

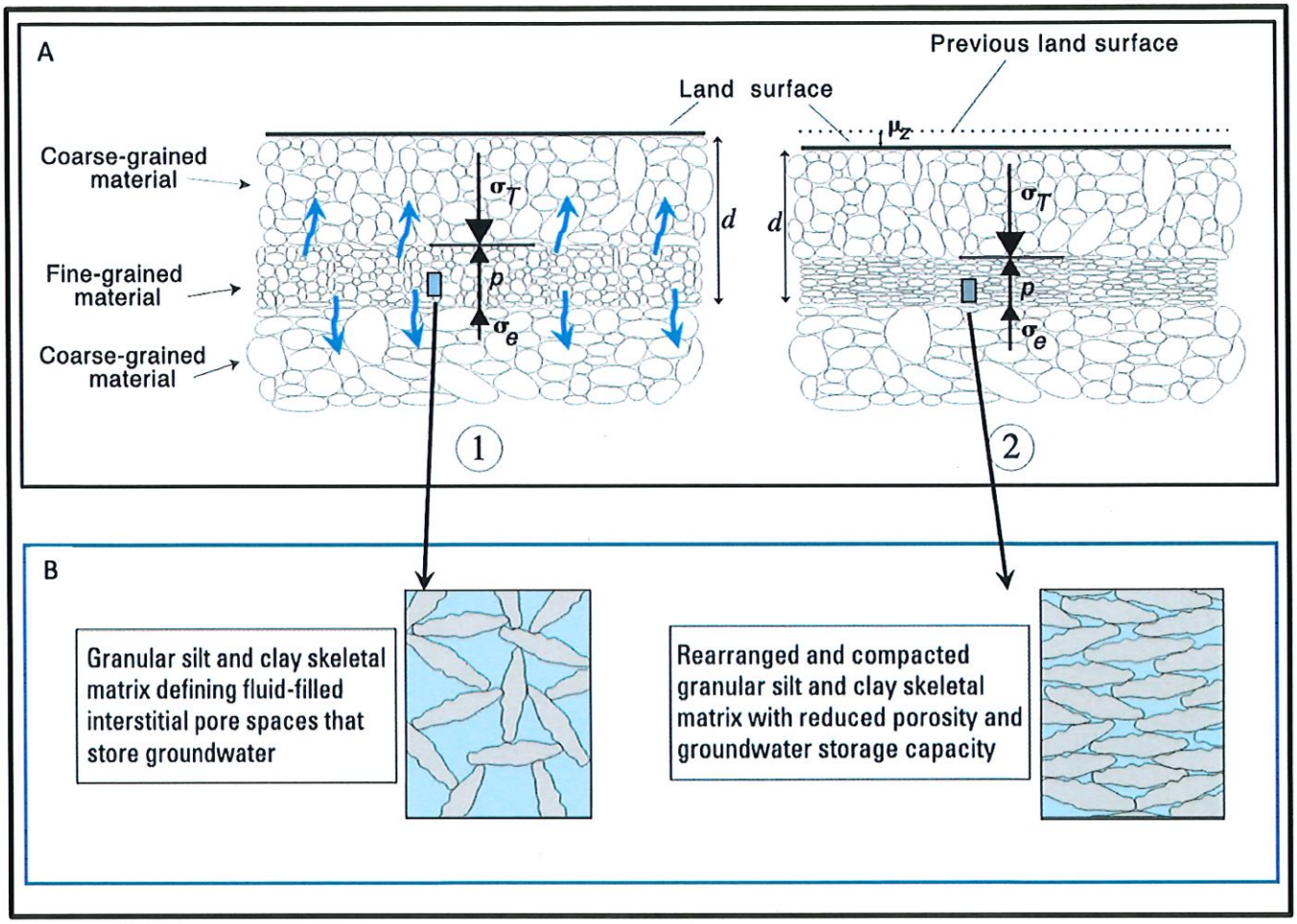

Figure 3. Simplified representation of the mechanisms of compaction land subsidence due to reduction in pore pressure by groundwater pumping. Modified from Figure 15 in Sneed, M. and Galloway, Devin L., 2000, Analyses and Simulations-the Holly Site, Edwards Air Force Base, Antelope Valley, California, U.S. Geological Survey Water-Resources Investigations Report 00-4015, 70 pp. Magnified view of sediment grains from diagram on Harris-Galveston Subsidence District website https://hgsubsidence.org/science-research/what-is-subsidence/

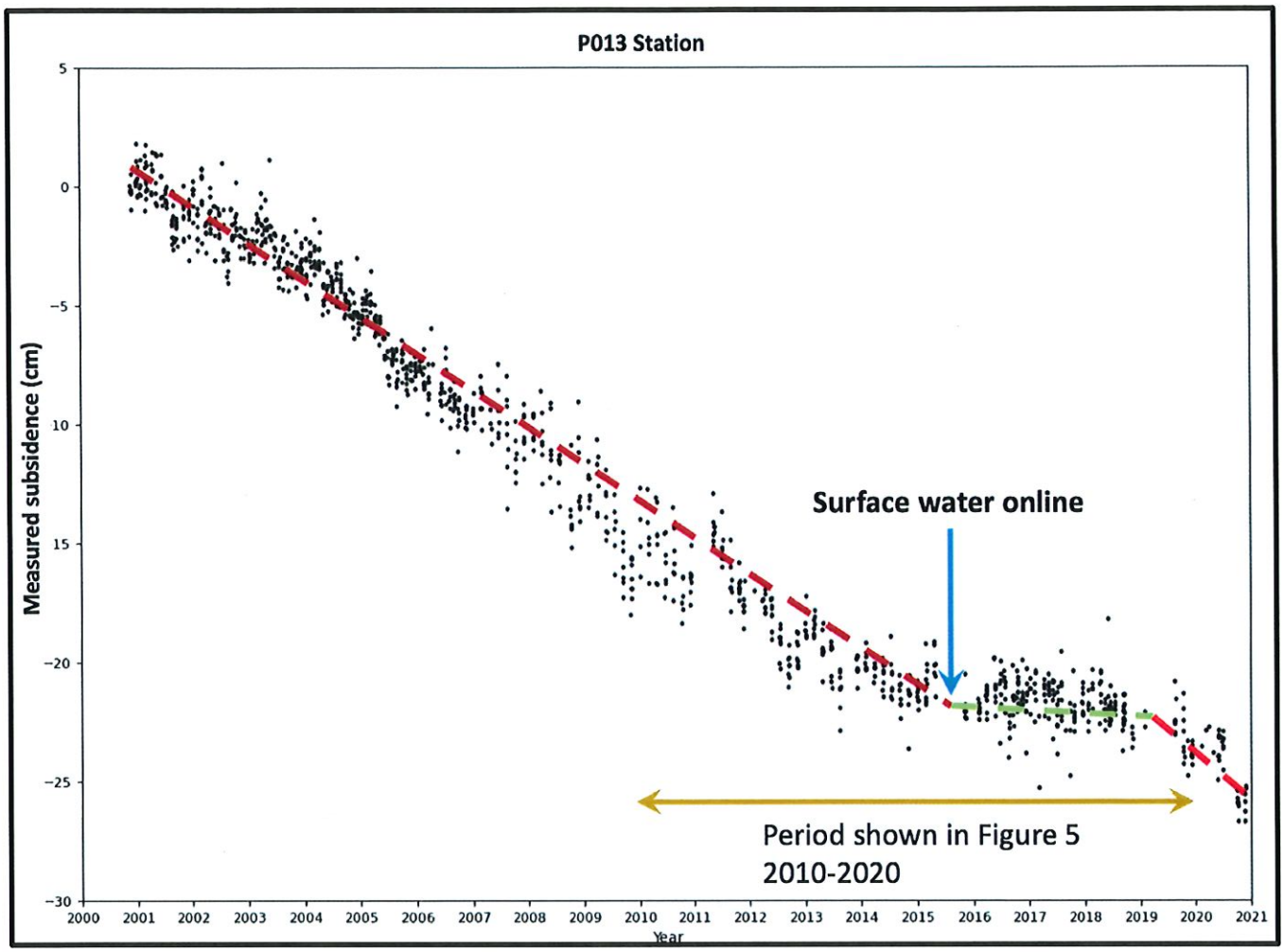

Figure 4. Plot of PAM 13 (P013) measured subsidence in The Woodlands. Lake Conroe surface water became available to The Woodlands in the latter half of 2015. For reference, the brown arrowed line shows the period represented in Figure 5. Plot retrieved from Interactive Map of Subsidence Rates at the Harris-Galveston Subsidence District website https://hgsubsidence.org/science-research/what-is-subsidence/

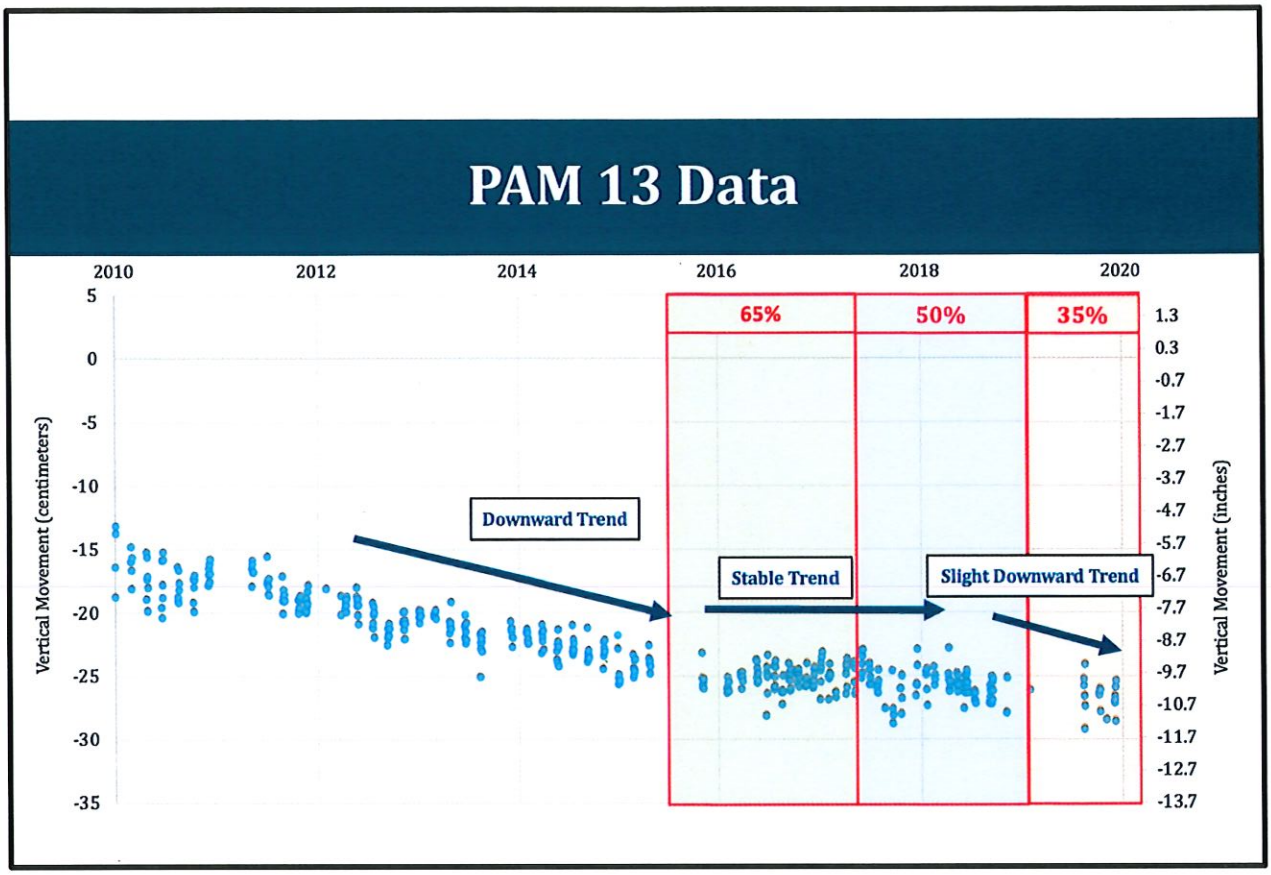

Figure 5. Detail of PAM 13 (P013) subsidence data over the period 2010 to the start of 2020. Figure from SJRA The Woodlands Division presentation 2020 Static Well Level Report, December 2020.

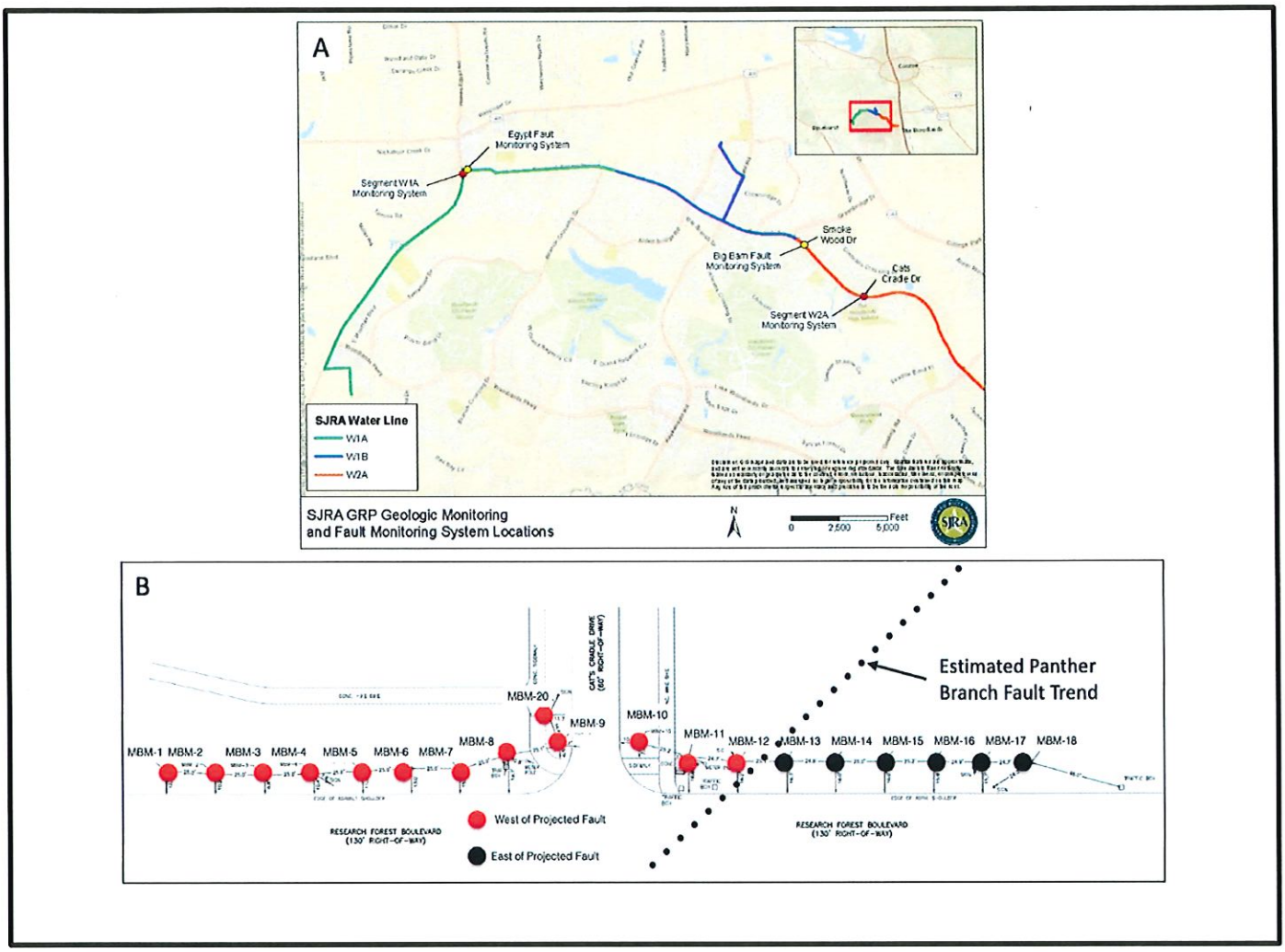

Figure 6.

A. Map of SJRA GRP Geologic Monitoring and Fault Monitoring System locations. Graphic from SJRA website https://www.sjra.net/grp/fault-monitoring/
B. Diagram provided by Dr. Mark Meinrath. Modified from graphic downloaded from SJRA website https://www.sjra.net/wp-content/uploads/2020/12/W2A-MONITORING-SURVEY_11-2020.pdf

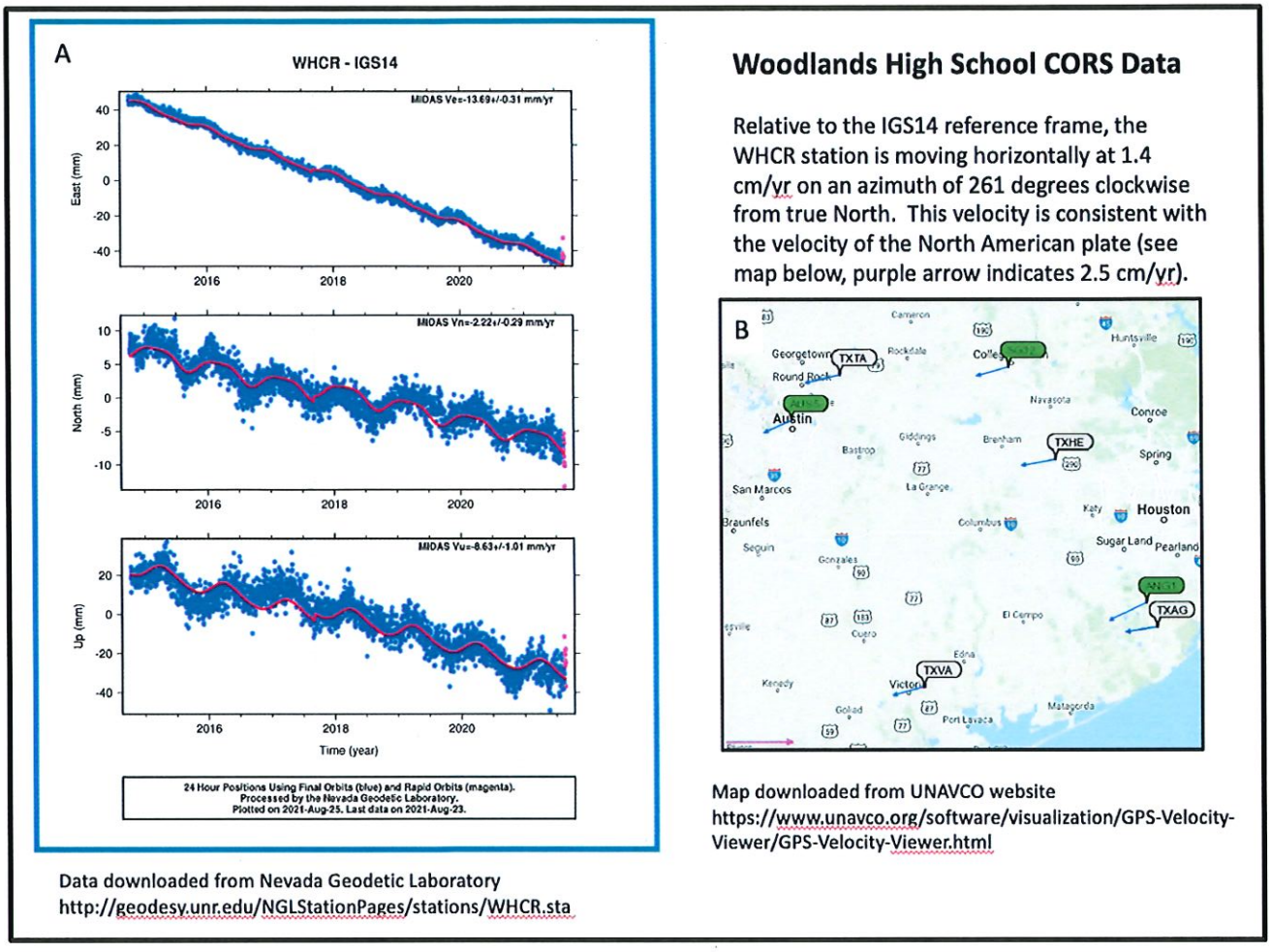

Figure 7.

A. CORS data from The Woodlands High School CORS site. Downloaded from the Nevada Geodetic Laboratory.
B. Map showing measured velocities for part of the North American plate in Texas. Downloaded from the UNAVCO website.

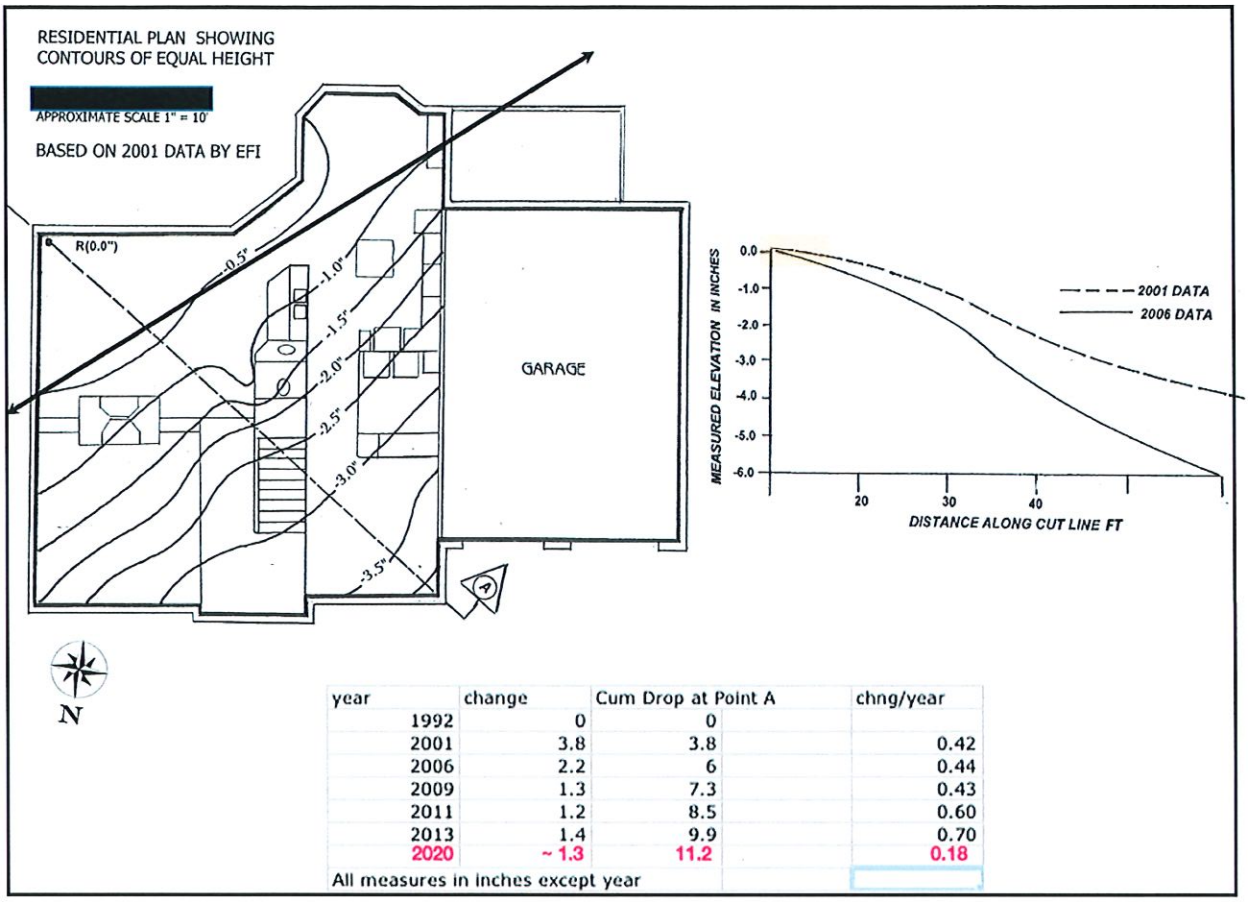

year	change	Cum Drop at Point A	chng/year
1992	0	0	
2001	3.8	3.8	0.42
2006	2.2	6	0.44
2009	1.3	7.3	0.43
2011	1.2	8.5	0.60
2013	1.4	9.9	0.70
2020	~ 1.3	11.2	0.18
All measures in inches except year			

Figure 8. Elevation survey results in plan and profile view of foundation deformation at the Meinrath residence. Measurements have been made since 2001. The estimated trace of the Panther Branch Fault is shown by the arrowed line on the plan of the residence. Dr. Meinrath provided the plan, profile and table showing the elevation changes over time. The address of the residence is obscured per Dr. Meinrath's request.

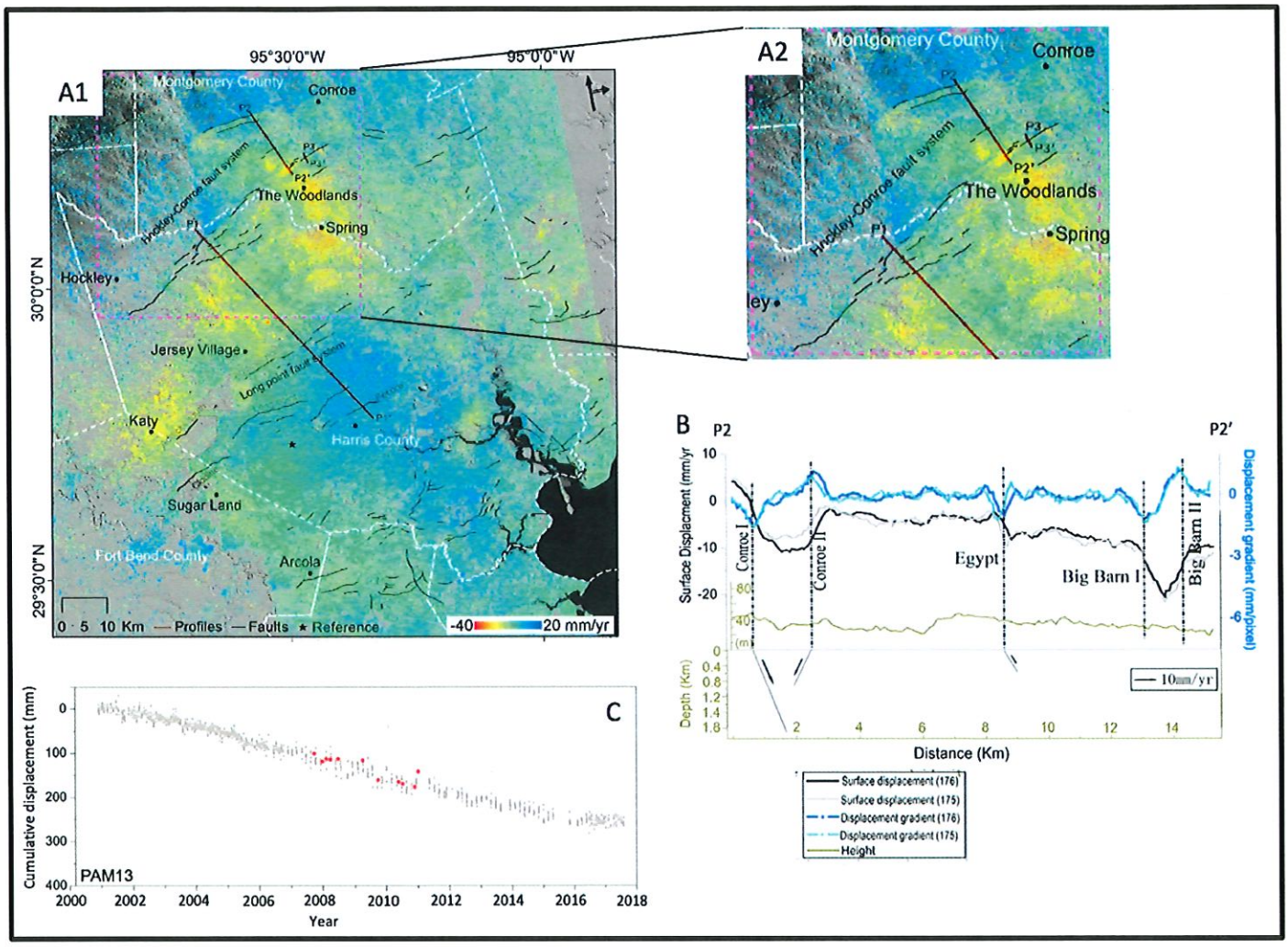

Figure 9.

A1. InSAR image of surface deformation for the period 2007 to 2011 over the Greater Houston area.

A2. Inset of image shown in Figure 9 A1 focusing on The Woodlands and adjacent areas. Profile line P2-P2' is in the upper part of the image.

B. Profile P2-P2' showing deformation gradient, surface displacement, topographic profile and results of geophysical analysis of fault geometry and displacement rate.

C. PAM 13 subsidence data (grey dots) over the period 2001 to 2018, with calibrated InSAR deformation data over the period 2007 to 2011.

Compiled from Figures 3 (a), 4, and 7 in Qu, et al., 2019. See text for full reference information.

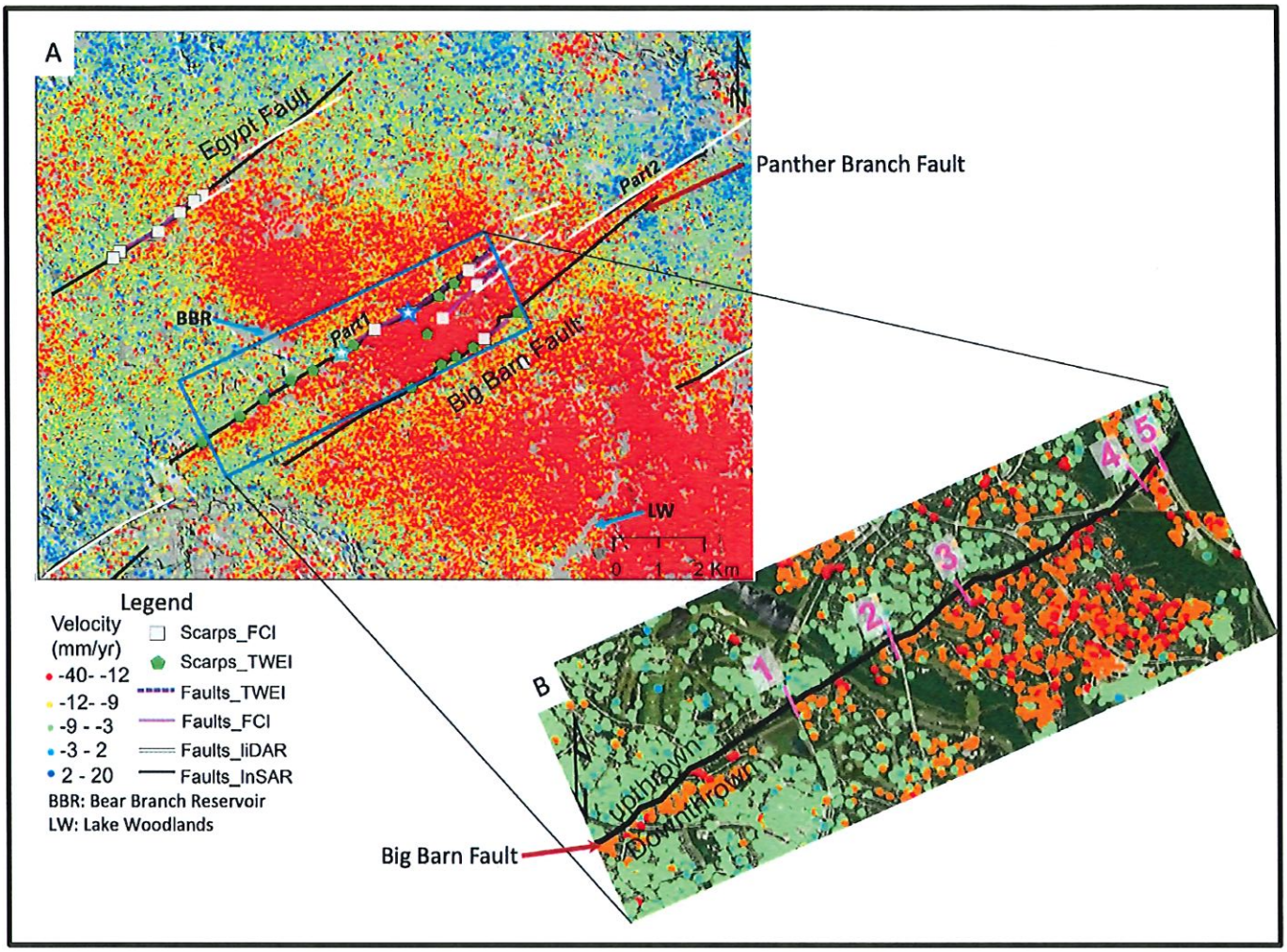

Figure 10.

A. Enlarged deformation map of the western part of The Woodlands showing the Egypt and Big Barn Fault complexes.
B. Detail of the Big Barn Fault.
Figure modified from Figure 6 in Qu, et al., 2019 (see text for full reference).